

Fluid Mixing Control Inside a Y-shaped Microchannel by Using Electrokinetic Instability *

Hui HU**, Zheyang JIN**, Abdulilah DAWOUD ***
and Ryszard JANKOWIAK ***

** Department of Aerospace Engineering, Iowa State University, Ames, Iowa 50011, USA.
E-mail: huhui@iastate.edu

***Department of Chemistry and Terry C. Johnson Center for Basic Cancer Research
Kansas State University, Manhattan, Kansas 66502, USA.

Abstract

A parametric study was conducted to improve our understanding pertaining to the fundamental physics of electrokinetic instability (EKI) and to explore the effectiveness of manipulating EKI waves to control/enhance fluid mixing inside a Y-shaped microchannel. The dependence of the critical strength of the applied static electric field to trigger the EKI waves on the conductivity ratio of the two mixing streams inside the Y-shaped microchannel was quantified at first. The effects of the applied electric field strength on the evolution of the EKI waves and the resultant fluid mixing were assessed in terms of scalar concentration distributions, shedding frequency of the EKI waves and fluid mixing efficiency. The effectiveness of manipulating the EKI waves by adding alternative perturbations to the applied static electric fields were also explored for the further enhancement of the fluid mixing inside the Y-shaped microchannel. The measurement results revealed that the relationship between the critical strength of the applied static electric field and the conductivity ratio of the two mixing streams in the Y-shaped microchannel can be represented well by a power function with the power index about -0.246. The fluid mixing efficiency was found to increase monotonically with the increasing strength of the applied electric field. The fluid mixing process was found to be further enhanced by adding alternative perturbations to the applied static electric fields with the mixing process being most enhanced when the frequency of the alternative perturbation is close to the natural shedding frequency of the EKI waves. The fluid mixing efficiency was found to increase rapidly as the amplitude of the alternative perturbation increases.

Key words: Electrokinetic Instability, Active Mixing Control in Microchannels, EKI Micro-Mixer, Epi-Fluorescence Imaging, Microfluidics

1. Introduction

Two-fluid mixing is an essential process for many microfluidic or “lab-on-a-chip” devices. Various biomedical and biochemical processes, such as DNA purification, polymerase chain reaction (PCR), enzyme reaction, and protein folding, involve the mixing of two fluids. The performance of such processes depends heavily on the mixing effectiveness and rapidness of the samples and reagents. However, effective mixing of two fluids inside microchannels could be very challenging since turbulence is usually absent due to the nature of low Reynolds numbers of the microflows. Therefore, studies aimed to develop novel techniques and methodologies to enhance diffusion-dominated fluid mixing

processes and to increase the interfacial contact surface area between adjacent streams inside microchannels are very important and necessary to improve the performance of microfluidic or “lab-on-a-chip” devices.

In recent years, extensive studies have been conducted to develop novel techniques and methodologies to enhance fluid mixing inside microchannels. Several innovative concepts of “micro-mixers” have been proposed through those studies. In general, the proposed “micro-mixers” can be categorized into two groups: passive mixers and active mixers⁽¹⁾. Passive mixers do not require external energy; the enhanced mixing process relies entirely on the augmentation of diffusion or chaotic advection through special geometrical design of microchannels. In contrast, active mixers usually rely on adding external energy to introduce disturbances to enhance fluid mixing; generating external disturbances in terms of temperature⁽²⁾, pressure⁽³⁾⁽⁴⁾, electrohydrodynamics⁽⁵⁾, dielectrophoretics⁽⁶⁾, acoustics⁽⁷⁾ as well as magnetohydrodynamics⁽⁸⁾, several kinds of active micro-mixers have already been proposed to effectively enhance fluid mixing in microchannels. In this study, we report a parametric study to quantify the effectiveness of achieving fluid mixing control/enhancement inside a Y-shaped microchannel using an active control method, electrokinetic instability (EKI).

EKI occurs when two streams with different electric conductivities meet in a microchannel under an applied static electric field as shown schematically in Fig. 1. If the strength of the applied static electric field exceeds a certain threshold value, the flow instability of adjacent streams could be observed in a sinuous form along the interface of the mixing streams⁽⁹⁾⁽¹⁰⁾. The conductivity gradient subject to an external electric field has been suggested as a source of electrical charges and the Coulombic force acts to generate additional body force⁽¹¹⁾. Relevant to the mechanism of electrokinetic instability, Hoberg & Melcher⁽¹¹⁾ showed that the interface of miscible fluids with conductivity gradient becomes unstable under a normal electric field in an unbounded domain. Baygents & Baldessari⁽¹²⁾ suggested that the flow generated in isoelectric focusing devices is a consequence of the free charges generated by the electric field applied normally to the conductivity gradient.

Oddy et al.⁽¹³⁾ is the first to use EKI to manipulate fluid mixing process in a microchannel. Chen et al.⁽¹⁰⁾ conducted a pioneer study to elucidate the underlying fundamental physics of EKI and associated flow phenomena in a T-shaped microchannel. They reported that EKI can be observed as convective waves propagating downstream as the strength of the applied static electric field exceeds a threshold value (i.e. the critical strength of the applied electric field called in the present study), which corresponds to the convectively unstable mode of the EKI. When the strength of the applied electric field becomes relatively high, upstream propagating waves were observed, indicating the mode of absolute instability. Chen et al.⁽¹⁰⁾ also suggested a physical model to capture the coupling between electric and flow fields. More recently, Posner & Santigao⁽¹⁴⁾ studied the behavior of EKI waves in a cross-shaped microchannel under a wide range of the applied static electric fields and conductivity ratios of the center-to-sheath streams. They found that the required critical strength of the applied static electric field depends on both the

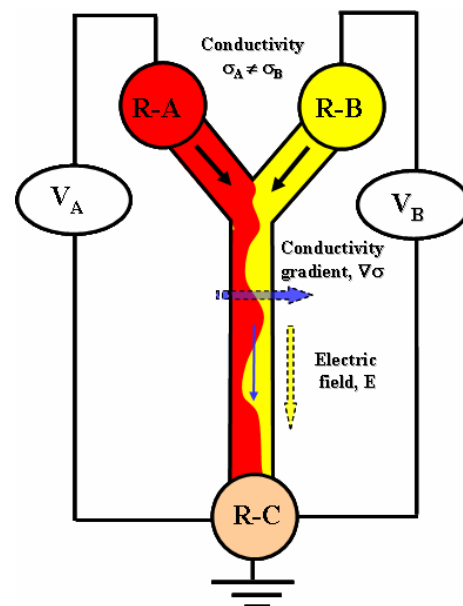


Fig.1. Schematic of EKI

centre-to-sheath conductivity ratio and the ratio of the static voltages applied to different branches of the cross-shaped microchannel. Shin et al.⁽¹⁵⁾ demonstrated for the first time that adding an alternative perturbation to the applied static electric field could manipulate EKI waves to either enhance or suppress the fluid mixing process in a cross-shaped microchannel depending on the frequency of the alternative perturbation.

Although many important results have already been obtained through those previous studies, much work is still needed to further our understanding about EKI and to explore/optimize design paradigms for the development of robust EKI micro-mixers for various microfluidics or “lab-on-a-chip” applications. For examples, so far, only Posner & Santigao⁽¹⁴⁾ conducted a parameter study to quantify the critical strength of the applied static electric field as a function of the conductivity ratio of the mixing streams in a cross-shaped microchannel. With the consideration of wide applications of two-stream mixing in Y-shaped microchannels instead of three-stream mixing in cross-shaped microchannels as the one used by Posner & Santigao⁽¹⁴⁾, the effects of the differences in the mixing flow arrangement (two-stream mixing vs. three-stream mixing, Y-shaped micro-mixers vs. cross-shaped micro-mixers) on the critical strength of the applied static electric field and the resultant fluid mixing process have never been explored. Although Shin et al.⁽¹⁵⁾ demonstrated the feasibility of adding alternative perturbations to the applied static electric fields to manipulate EKI waves to control fluid mixing process, very little in the literature can be found to quantify the effect of relevant parameters such as the frequency and amplitude of the alternative perturbations on the evolution of the EKI waves and the resultant fluid mixing efficiency. With these in mind, we conducted the present study to further our understanding about the fundamental physics of EKI and to explore/optimize design paradigms for the development of robust EKI micro-mixers for various microfluidics or “lab-on-a-chip” applications.

In the present study, a parametric study was carried out to elucidate underlying physics and to quantify the effectiveness of manipulating EKI waves to actively control/enhance fluid mixing inside a Y-shaped microchannel. Epi-fluorescence imaging technique was used to conduct qualitative flow visualization and quantitative scalar concentration field measurements to quantify the fluid mixing process inside the Y-shaped microchannel in terms of scalar concentration distribution, shedding frequency of the EKI waves and scalar mixing efficiency. The effects of the relevant parameters, such as the conductivity ratio of the two mixing streams, the strength of the applied static electric fields, and the frequency and amplitude of the applied alternating perturbations, on the evolution of the EKI waves and resultant fluid mixing process were investigated systematically.

2. Experimental Details

The Y-shaped microchannel used in the present study is made of poly-di-methyl-siloxane (PDMS) by using a rapid-prototyping “photolithography” technique⁽¹⁶⁾. The dimensions of the microchannel are given in Fig. 2. The cross section of the channel is rectangular with 320 μm in width and 130 μm in height. The length of both inlet branches is 15.0mm, and the angle between the two inlet branches is 90°. The length of the mixing channel is 40.0mm. Relatively large reservoirs at the inlets and outlet of the Y-shaped microchannel are designed in order to minimize the effect of the induced

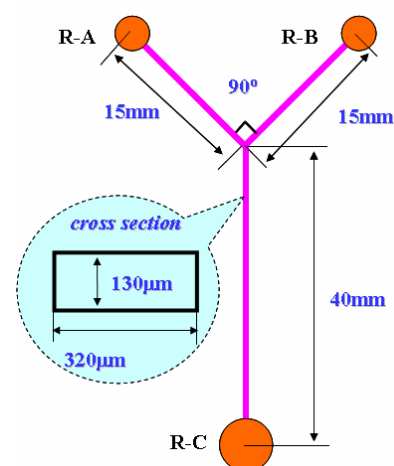


Fig. 2. The schematic of the Y-shaped microchannel

pressure head difference between the inlets and outlet during the experiments.

Deionized water was used as the working fluid in the present study. The DI water was filtered by using a syringe filter unit (Millipore millex-FG, Bedford, 0.2 μ m) before experiments. Borate buffers (Science Stuff Inc) were used to adjust the molecular conductivity of the two fluid streams. Rhodamine B, which is reported to be neutral for pH values ranging 6.0 to 10.8⁽¹⁷⁾, was used as the fluorescent dye for qualitative flow visualization and quantitative scalar concentration measurements. Since the molar concentrations of the borate buffers (<10mM) and Rhodamine B (<0.16 mM) are low, the changes in water physical properties such as the permittivity and viscosity are negligible. DI water was used to flush the microchannel several times prior to use for experiments.

Figure 3 shows the schematic of the experimental setup used in the present study. The microchip with the Y-shaped microchannel was placed on the test bed of an inverted fluorescent microscope (Leica DM-IL). A high-voltage DC power supply (Keithley, Model 247) was used to provide a static electric field between the reservoirs R-B and R-C. A function generator (Instek, Model GFG-8250A) and a high-voltage amplifier (Trek, Model 609-E) were used to apply static electric field or a static electric field along with an alternating perturbation between the reservoirs R-A and R-C. The electrodes installed in the reservoirs are made of platinum.

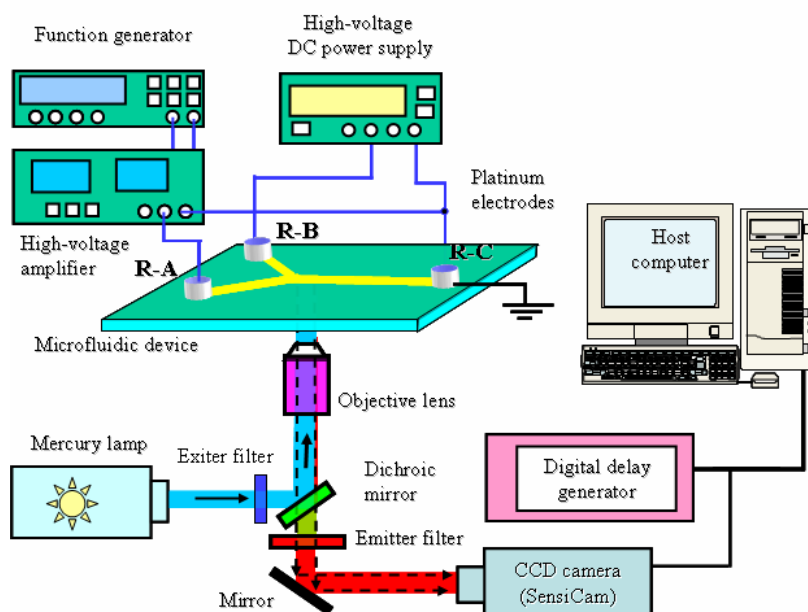


Fig. 3. Experimental setup

A mercury lamp was used as the illumination source in the present study. Passing through an epi-fluorescent prism (Excitation Filter of 532nm with 10nm BP, Dichroic 532nm RDC, Emitter of 610nm with 75 nm BP), the bright light from the mercury lamp was used to excite the Rhodamine B molecules seeded in the stream R-A. Upon excitation, the seeded fluorescent tracer, Rhodamine B molecules, would emit fluorescence with its emission peak at about 580nm. A 10X objective lens (NA=0.4) was used for the fluorescence imaging. The fluorescence light was captured by a high-resolution CCD camera (SensiCam-QE, Cooke Corp). The CCD camera was connected to a workstation (host computer) via a digital delay generator (Berkeley Nucleonics, Model 565) for the image acquisition timing control, data storage and imaging processing. For the present study, the exposure time of the CCD camera was set at 7ms. 500 fluorescence images were recorded at a frame rate of 10 Hz for each case.

It should be noted that the depth averaging along the optical axis is an artefact of epi-fluorescence imaging to study microflows. All the fluorescent molecules across the

imaging depth of the 10X objective would contribute to the measured fluorescence intensity. Based on the formula suggested by Inoue & Spring⁽¹⁸⁾, the depth of focus for the 10X (NA=0.4) objective used in the present study is estimated to be about 5.0 μm . For all the experimental results reported here, the focus plane of the 10X objective was set in the middle plane of the 130 μm depth microchannel.

It is well known that the collected fluorescence intensity is proportional to the amount of the fluorescent molecules in the flow for diluted solution and unsaturated excitation. Quantitative scalar concentration distributions can be derived from the acquired fluorescence images. In the present study, a calibration experiment was conducted to confirm the linear relationship between the collected LIF signal and the concentration of the seeded Rhodamine B molecules. Following the similar procedure as described by Hu et al.⁽¹⁹⁾ and Posner & Santiago⁽¹⁴⁾, the effects of the non-uniformity of the illumination intensity, background noise, and the dark current of the CCD camera were corrected in the present study in order to minimize the measurement errors in the determination of scalar concentration distributions to quantify the scalar mixing process. In the present study, the size of the field of view is about 0.6 mm by 2.0mm with the spatial resolution of the acquired LIF images about 1.45 $\mu\text{m}/\text{pixel}$. Based on the calibration profile and signal-noise-ratio of the acquired LIF images, the uncertainty for the concentration distribution measurement results given in the present study was estimated to be within 2.0%.

3. Quantification of Fluid Mixing Effectiveness

Following the work of Johnson et al.⁽²⁰⁾, a statistical approach was used in the present study to quantify the fluid mixing process in the Y-shaped microchannel. After a procedure was conducted to correct the effects of the non-uniformity of the illumination intensity, background noise and the dark current of the CCD camera, the acquired fluorescence images were used to calculate the fluid mixing efficiency, η , which is defined as:

$$\eta = 1 - \frac{\sqrt{\frac{1}{N} \sum_{i=1}^N (I_i - I_{ip})^2}}{\sqrt{\frac{1}{N} \sum_{i=1}^N (I_{io} - I_{ip})^2}}$$

where N , I_i , I_{io} and I_{ip} represent the total number of pixels, fluorescence intensity at the i th pixel, the fluorescence intensity at the i th pixel without any mixing or diffusion, and the fluorescence intensity at the i th pixel for homogenous mixtures, respectively.

When the two streams are perfectly mixed, every pixel should of course have the same intensity equal to the averaged value of all partially mixed pixel intensities, i.e.,

$$I_{ip} = \frac{1}{N} \sum_{i=1}^N I_i$$

On the other hand, if the two streams do not mix at all, half of the pixels that belong to the dark stream should have zero-intensity, while the other half in the fluorescent stream should have an intensity of I_{io} . Thus, I_{io} distribution was determined by setting the image intensity of the bright half of the channel to $2 I_{ip}$ and the opposite of the channel to zero. The mixing efficiency, η , ranges from 0 to 1 with $\eta=1$ indicating complete mixing, and $\eta=0$ no mixing.

It should be noted that, although the measurement results given in the present paper were mainly based on the measurements in the middle plane of the 130 μm microchannel, a series of concentration measurements were also conducted at 5 different locations along the depth of the microchannel (from -60 μm to +60 μm off the middle plane) for some selected cases. It was found that the flow field was quite two-dimensional along the depth of the microchannel with the variation of the time-averaged mixing efficiency within 2.0% in different measurement planes.

4. Experimental Results and Discussions

1. The effect of conductivity ratio of the two mixing stream in the Y-shaper michrochannel on the critical strength of the applied static electric field.

Chen et al. ⁽⁹⁾ reported that EKI would be observed in forms of convective waves propagating downstream when the strength of the applied static electric field exceeds a certain threshold value, i.e., there exists a required minimum strength of the applied electric field in order to trigger the shedding of the convective EKI waves. So far, only Posner & Santigao ⁽¹⁴⁾ conducted a parameter study to quantify the critical strength as a function of the conductivity ratio of the centre-to-sheath streams and the ratio of the static electric strength applied to different branches of a cross-shaped microchannel for a three-streams mixing application. Much work is still needed in order to establish a database for theoretic modeling and prediction of EKI and associated flow phenomena for various microfluidics or “lab-on-a-chip” applications. More specifically, with the considerations of wide applications of two-streams mixing and simple geometry of Y-shaped micro-mixers, the dependence of the critical strength on the conductivity ratio of the two mixing streams in Y-shaper microchannels has never been systematically investigated.

In the present study, we conducted a parametric study to quantify the effect of the conductivity ratio of the two mixing streams on the critical strength of the applied static electric field to trigger EKI waves in a Y-shaped microchannel. During the experiments, the concentration of borate buffer solution in inlet reservoir R-B was kept as constant at 10mM, the concentration of the borate buffer in inlet reservoir R-A was changed from 0.1mM to 5mM. It makes the conductivity ratio of the two mixing streams, $\gamma = \sigma_B / \sigma_A$, being 2:1, 5:1, 10:1, 50:1 and 100:1. Rhodamine B molecules were seeded in the stream R-A to visualize the evolution of the interface of the two mixing streams.

In order to determine the critical strength of the applied static electric field to trigger the periodic shedding of convective EKI waves at a selected conductivity ratio, a small static voltage was applied between the inlets and outlet of the Y-shaped microchannel at first. Then, the applied voltage was increased in the step of every 25 volts until noticeable fluctuations of the interface of the two adjacent streams can be observed. During the experiments, the same static voltage was applied to both inlet reservoirs R-A and R-B at all times, i.e., $V_A = V_B$. The required minimum voltage to induce observable fluctuations at the interface of the two adjacent streams is defined as the critical voltage of the applied electric field at that selected conductivity ratio.

Figure 4 shows the measured critical strength of the applied static electric field as a function of the conductivity ratio of the two mixing streams inside the Y-shaped microchannel. A curve of a power function is also given in the figure to fit the measurement data. It can be seen clearly that the critical strength of the applied static electric field decreases rapidly (the power index of the power function is -0.246) with the increasing conductivity ratio. The critical strength was found to be about $E_{critical} \approx 160 \text{ Vcm}^{-1}$ as the conductivity ratio being 2. It drops to about $E_{critical} \approx 60 \text{ Vcm}^{-1}$ as the conductivity ratio increases to 100. This can be explained by that a larger conductivity ratio would induce a higher free charge density, ρ_e , as suggested by

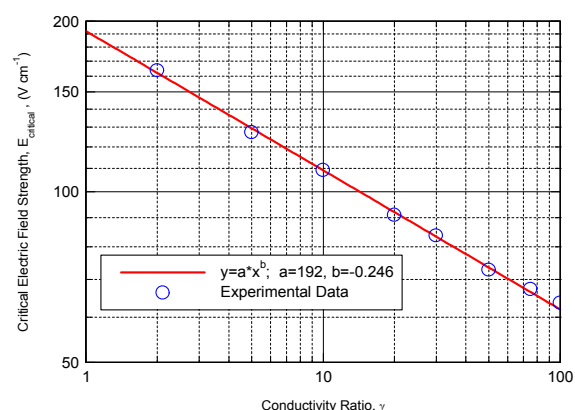


Fig. 4. Critical strength of the applied electric field vs. conductivity ratio

Hoberge & Melcher⁽¹¹⁾ with a relationship of $\rho_e = -\frac{\varepsilon}{\sigma} \nabla \sigma \cdot E$, where σ the electrical conductivity of the fluid, ε the electrical permittivity of the fluid, and E the external electric field. The greater induced electric charges coupled with the applied electric field would generate a stronger Coulombic force at the interface of the two adjacent streams to overcome the dissipative effects of the molecular diffusion to promote EKI. Therefore, the critical strength would decrease rapidly with the increasing conductivity ratio of the two mixing streams in the Y-shaped microchannel.

It should be noted that, although Posner & Santigao⁽¹⁴⁾ reported a similar trend about the dependence of the critical strength of the applied static electric field on the conductivity ratio of the mixing streams, the present study is the first to reveal that the relationship can be represented well by a power function. It should also be noted that the absolute values of the critical strength for the present study (i.e., for two-streams mixing in the Y-shaped tunnel) were found to be much smaller than those reported by Posner & Santigao⁽¹⁴⁾ (for three-stream mixing in a cross-shaped microchannel). For example, for the same conductive ratio of $\gamma = 10$, the critical strength of the applied electric field to trig EKI waves in the Y-shaped microchannel is $E_{critical} \approx 110 \text{ Vcm}^{-1}$ for the present study. Posner & Santigao⁽¹⁴⁾ reported that the critical strength would be as high as $E_{critical} \approx 420 \text{ Vcm}^{-1}$ in order to trigger EKI waves for the three-stream mixing in the cross-shaped microchannel. This indicates that the required strength of the applied static electric field would be affected by many other factors as well, in addition to the conductivity ratio of the mixing streams. It highlights the necessity of much more systematic studies to establish a comprehensive database to document EKI and associated flow phenomena in order to further our understanding about EKI and to explore/optimize design paradigms for the development of robust EKI micro-mixers for various microfluidics or “lab-on-a-chip” applications.

Figure 5 shows typical instantaneous fluorescence images of the fluid mixing inside the Y-shaped channel under the same applied static electric fields of $E \approx 180 \text{ Vcm}^{-1}$, however, with different conductivity ratio of the two mixing streams. Even though the strength of the applied electric field was kept constant, the fluid mixing process was found to become more and more turbulent and intensive as the conductivity ratio increases, i.e., the fluid mixing process was found to be enhanced significantly as the conductivity ratio of the two mixing streams increases.

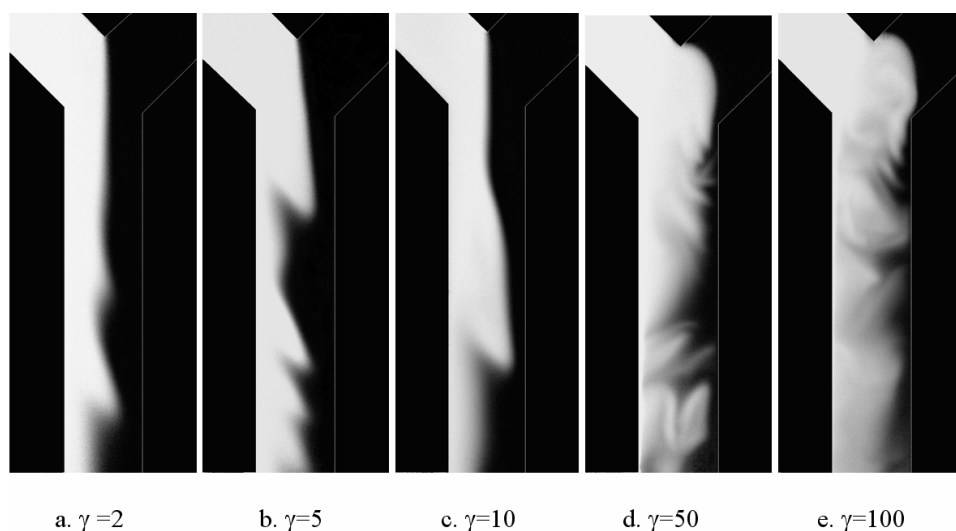


Fig. 5. The effect of the conductivity ratio on the fluid mixing process.

2. The effect of the applied electric field strength on the evolution of EKI waves

We also conducted a systematic study to investigate the effect of the strength of the applied electric field on the evolution of the EKI waves and the fluid mixing process inside the Y-shaped microchannel. During the experiment, the conductivity ratio of the two mixing streams is kept constant, i.e., $\gamma = 10$. The same static voltages were applied to both the inlet reservoirs R-A and R-B, i.e., $V_A = V_B$, with the applied voltage varied from 100V to 2000V (i.e., $E \approx 18 \sim 365 \text{ Vcm}^{-1}$).

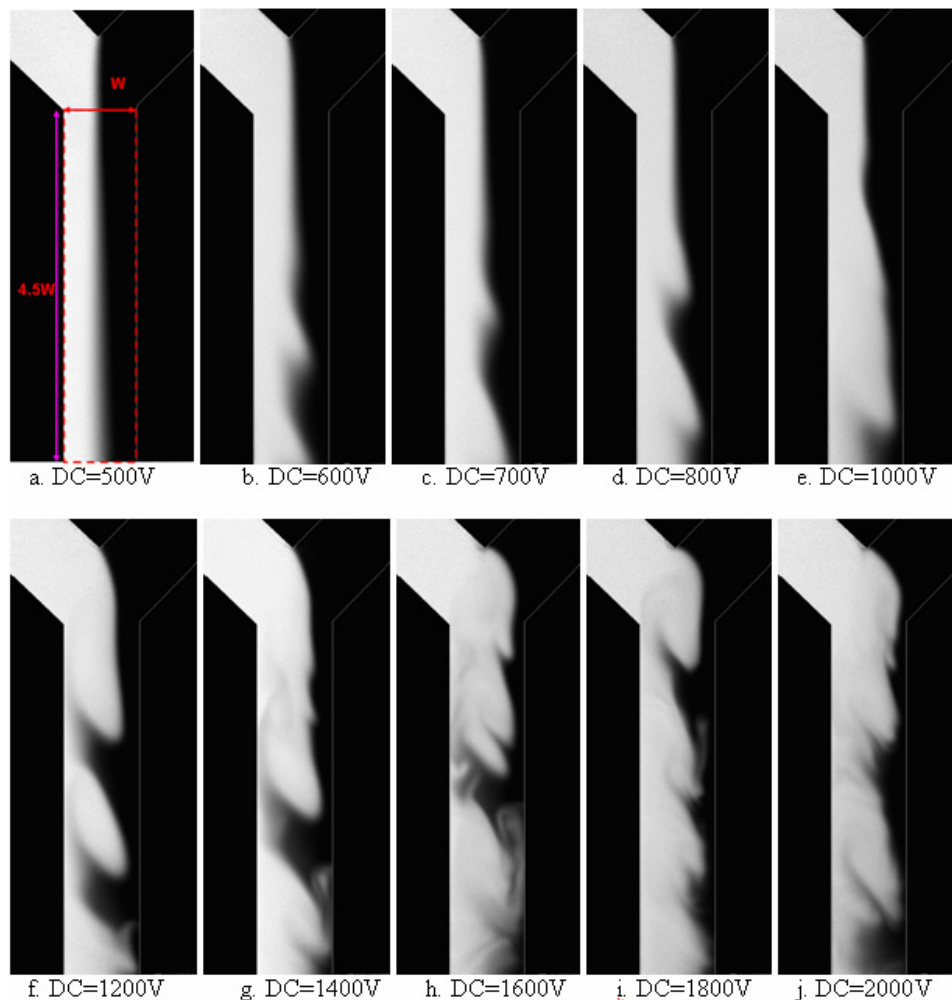


Fig. 6. The effect of the applied electric field strength on the fluid mixing ($\gamma = 10$)

Figure 6 shows typical fluorescence images under different strengths of the applied static electric field. As visualized clearly in the images, the interface of the two adjacent streams was found to be straight and “clean” as the applied static voltage is relatively low (i.e., $< 550\text{V}$). No noticeable fluctuations of the interface of the two mixing streams can be observed. The fluid mixing was found to concentrate in a very thin layer along the straight interface of the two streams, and the fluid mixing process was found to be diffusion dominated. As the applied voltage becomes greater than 550V (i.e., $E > 110 \text{ Vcm}^{-1}$), the interface was found to fluctuate and generate observable convective EKI waves, which were found to propagate downstream. The generation of the convective waves was found to be periodic. The shedding frequency of the EKI waves can be identified from the scalar temporal power spectra based on the time sequence of the captured fluorescence images, and the results are given in Fig. 7. The amplitude of the interface fluctuation, i.e., the size of the convective EKI waves, was found to increase rapidly as the applied static voltage increased. When the applied static voltage is less than 1000V (i.e., $E < 180 \text{ Vcm}^{-1}$), the interface of the

two mixing streams was found to be “clean” and “laminar” while it was curved due to the periodic shedding of the EKI waves. The shedding frequency of the EKI waves was found to decrease with the increasing voltage of the applied static electric field when the applied static voltage is relatively low (i.e., $E < 180 \text{ V cm}^{-1}$).

As the applied static voltage becomes higher than 1000V (i.e., $E > 180 \text{ V cm}^{-1}$), additional smaller EKI waves were found to be generated in the braid regions of the large convective EKI waves. The smaller EKI waves were found to propagate upstream instead of downstream. Due to the generation of the additional smaller EKI waves, the shedding frequency of the convective EKI waves was found to increase slightly with the increase of

the applied static voltage. The generation of the convective EKI waves became much more random, and the interface of the adjacent streams became much “dirtier” and fussier when the applied static voltage is higher than 1200V (i.e., $E > 218 \text{ V cm}^{-1}$). As the applied static voltage becomes higher than 1400V (i.e., $E > 255 \text{ V cm}^{-1}$), the fluid mixing process in the microchannel was found to become much more turbulent and chaotic. The scalar temporal power spectra based on the time sequence of the fluorescence images were found to become continuous energy spectra, and no obvious peak can be identified when the applied static voltage become larger than 1600V (i.e., $E > 290 \text{ V cm}^{-1}$).

In order to quantify the effect of the strength of the applied static electric fields on the fluid mixing process inside the microchannel more clearly, fluid mixing efficiency under different strengths of the applied electric field were calculated. The interrogation area used for the fluid mixing efficiency calculation is shown in Fig 6 (a), and the calculated fluid mixing efficiency data are given in Fig. 8. It can be seen clearly that the fluid mixing efficiency increase monotonically with the increasing strength of the applied static electric field.

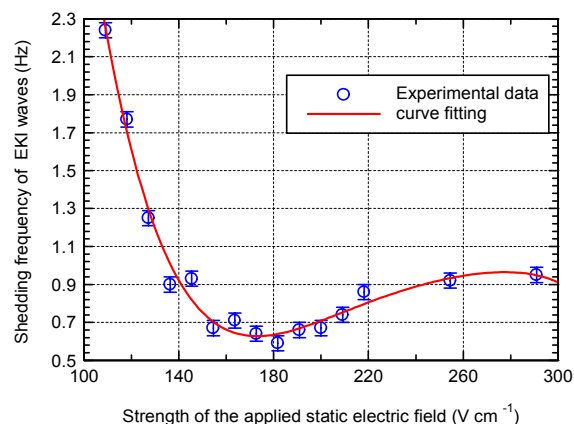


Fig. 7. The shedding frequency of convective EKI waves versus the applied static voltage

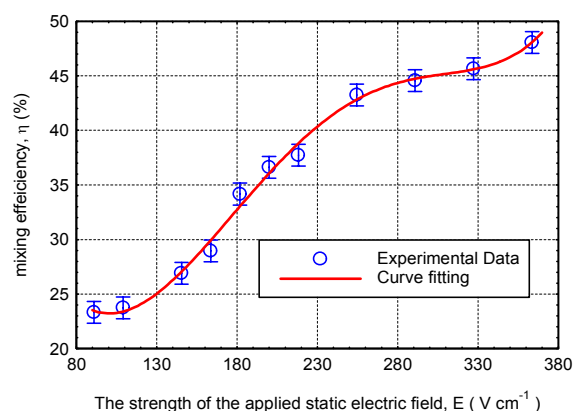


Fig. 8. Mixing efficiency vs. the strength of the applied static electric field

3. Manipulating the EKI waves and fluid mixing process by adding alternative perturbation to the applied static electric field.

Although Shin et al.⁽¹⁵⁾ demonstrated the feasibility of adding alternative perturbations to applied static electric fields to manipulate EKI waves for fluid mixing control, the effects of relevant parameters such as the frequency and amplitude of the alternative perturbation on the evolution of EKI waves and the resultant fluid mixing have not been fully investigated. In the present study, we conducted a systematic investigation to quantify the effectiveness of adding alternative perturbations to the applied static electric field to

manipulate EKI waves for further enhancement of fluid mixing in the Y-shaped microchannel. During the experiments, while the same static voltage of 1000V was applied to the inlet reservoirs R-A and R-B, an alternative perturbation was added to the inlet reservoir R-A. Therefore, the voltages applied to the inlets of the Y-shaped microchannel were:

$$\begin{aligned} V_A &= V_{DC} + \tilde{V}_{AC} = V_{DC} + A_{AC} \sin(2\pi f_{AC}) = 1000V + \sin(2\pi f_{AC}); \\ V_B &= V_{DC} = 1000V \end{aligned}$$

By changing the frequency, f_{AC} , and amplitude, A_{AC} , of the alternative perturbation, the effects of the applied alternative perturbation on the evolution of the EKI waves and the resultant fluid mixing efficiency in the Y-shaped microchannel were assessed.

A mixing augmentation factor is introduced in the present study to quantify the augmentation in fluid mixing due to the addition of the alternative perturbation to the applied static electric field. The mixing augmentation factor, MAF , is defined as:

$$MAF = \frac{\eta_{static + perturbation}}{\eta_{static only}}$$

where $\eta_{static only}$ is the fluid mixing efficiency for the case without the alternative perturbation. $\eta_{static + perturbation}$ represents the fluid mixing efficiency when the alternative perturbation was added to the applied static electric field. $MAF > 1.0$ indicates that the fluid mixing process is enhanced by adding an alternative perturbation to the applied static electric field, while $MAF < 1.0$ represents that the fluid mixing process is suppressed by the addition of the alternative perturbation.

3a. The effect of the frequency of the alternative perturbation

During the experiment, the amplitude of the alternative perturbation was kept constant, i.e., $A_{AC} = 250V$. The frequency of the applied alternative electric perturbation was changed from 0.1 Hz to 100 Hz.

According to the experimental data given in Fig. 7, the shedding frequency of the EKI waves under a static voltage of 1000V ($E \approx 182 Vcm^{-1}$) between the inlets and the outlet of the Y-shaped microchannel was 0.60 Hz (i.e., $f_{DC} = 0.60Hz$). Figure 9 shows the mixing augmentation factor as a function of the frequency of the alternative perturbation. While Shin et al. ⁽¹⁵⁾ suggested that adding alternative perturbation to applied static electric field can both enhance and suppress fluid mixing of three fluid streams in a cross-shaped microchannel, depending on the frequency of the added alternative perturbation. The measurement results of the present study given in Figure 9 indicate clearly that the fluid mixing of the two fluid streams in the Y-shaped microchannel can always be enhanced by adding the alternative perturbation to the applied static electric field.

The mixing augmentation factor was found to reach its peak value as the frequency of the alternative perturbation is about 0.6Hz, which is close to the natural shedding frequency of the EKI waves under the applied static electric field of 1000V ($E \approx 182 Vcm^{-1}$). When the frequency of the applied alternative electric perturbation is too high ($f_{AC} > 10$ Hz) or too low ($f_{AC} < 0.1$ Hz) compared with the natural shedding frequency of the EKI waves, the applied alternative perturbations

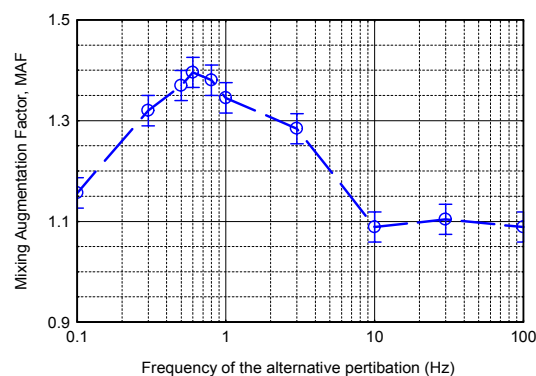


Fig. 9. Mixing augmentation factor vs. the frequency of the alternative perturbation.

were found to be able to barely affect the evolution of the convective EKI waves, therefore, the mixing augmentation factor was found to be slight bigger than 1.0.

The measurement results of the present study indicate clearly that the fluid mixing process inside the Y-shaped microchannel could be most enhanced when the frequency of the applied alternative perturbation equals to the natural shedding frequency of the EKI waves. This fact may be explained by the concept of hydrodynamic resonance, which has been widely employed in many active flow control studies⁽²¹⁻²²⁾. The existence of the optimal perturbation frequency is expected to provide a valuable guideline for the design of an EKI micro-mixers for efficient fluid mixing inside microchannels.

It should be noted that Shin et al.⁽¹⁵⁾ suggested that the optimum frequency for the applied alternative perturbation should be twice of the natural shedding frequency of the convective EKI waves when they studied the fluid mixing of three streams in a cross-shaped channel. The inconsistency about the optimum frequency of the alternative perturbation between the present study and Shin et al.⁽¹⁵⁾ is believed to be closely related to the differences in mixing flow arrangement (two-stream mixing vs. three-stream mixing) and number of interfaces (one high-conductivity-gradient layer vs. two high-conductivity-gradient layers) involved in the two studies.

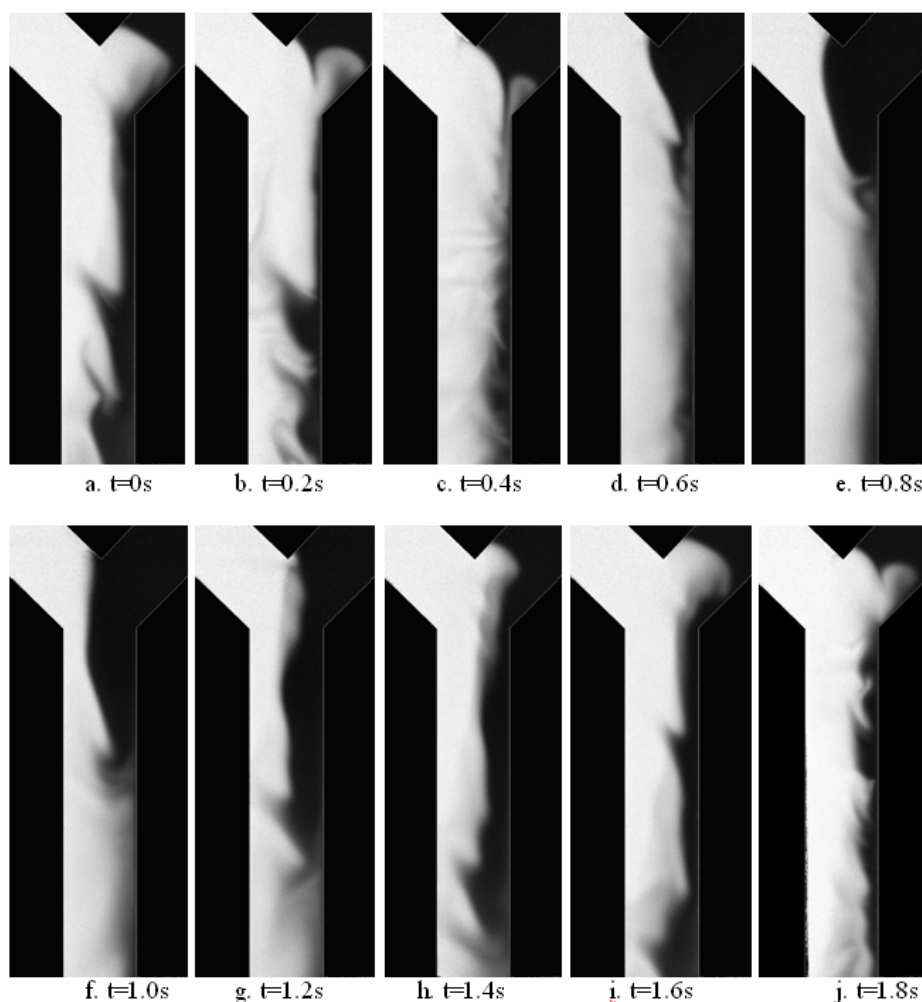


Fig. 10. Time sequence of the fluorescence images within one cycle of the alternative perturbation ($f_{AC}=0.60\text{Hz}$)

Figure 10 shows the time sequence of the fluorescence images within one excitation cycle of the applied alternative perturbation with the frequency of the perturbation being 0.60Hz. The evolution of the EKI waves and the dynamics of the EKI mixing process under

the excitation of the alternative perturbation were revealed clearly from the time sequence of the fluorescence images.

3b. The effect of the amplitude of the alternative perturbation on the evolution of the EKI waves and resultant fluid mixing process

While Shin et al.⁽¹⁵⁾ demonstrated the feasibility of manipulating EKI waves to control fluid mixing inside a cross-shaped microchannel by adding an alternative perturbation to the applied static electric field; the effects of the amplitude of the alternative perturbation on the evolution of EKI waves and resultant fluid mixing process have never been systematically investigated. We conducted a parametric study to quantify the effect of the amplitude of the alternative perturbation on the evolution of the EKI waves and resultant fluid mixing in the Y-shaped microchannel. The work presented at here is believed to be the first effort of its nature.

Since the fluid mixing process was found to be most enhanced when the frequency of the applied alternative perturbation is close to the natural shedding frequency of the EKI waves. Therefore, the frequency of the alternative perturbation was set to be the natural shedding frequency of the EKI waves (0.60 Hz) when we studied the effect of the amplitude of the alternative perturbation on the evolution of the EKI waves and the resultant fluid mixing process. During the experiment, we chose the parameters of $V_{DC}=1000V$, $f_{AC}=0.60Hz$. The amplitude of the alternative perturbation was changed from 50V to 500V.

Figure 11 shows the profile of the measured mixing augmentation factor versus the amplitude of the alternative perturbation. It can be seen clearly that the fluid mixing efficiency is quite sensitive to the amplitude of the alternative perturbation. The mixing augmentation factor was found to increase almost linearly with the amplitude of the applied alternative perturbation when the perturbation amplitude is relatively small (<200V). The fluid mixing efficiency was found to increase much more rapidly as the perturbation amplitude becomes relatively large (> 200V).

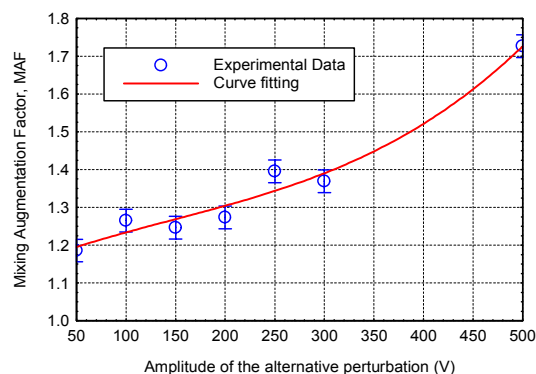


Fig. 11. *MAF* versus the amplitude of the alternative perturbation

5. Conclusions

A parametric study was carried out to elucidate underlying physics of electrokinetic instability (EKI) and to quantify the effectiveness of manipulating EKI waves to actively control/enhance fluid mixing inside a Y-shaped microchannel. The critical strength of the applied static electric field, which is the required minimum strength of the applied electric field to “trigger” the generation of EKI waves at the interface of the mixing streams, was found to heavily depend on the conductivity ratio of the mixing streams in the Y-shaped channel. The measurement results of the present study revealed that the relationship between the critical strength of the applied static electric field and the conductivity ratio of the two mixing streams could be represented well by a power function. The evolution of the EKI waves was found to change greatly with the increasing of the applied electric field strength. As the strength of the applied electric field is relatively weak, the EKI waves were found to propagate downstream with their size growing rapidly with the increasing strength of the applied static electric field. Additional smaller EKI waves were found to form in the

braid regions of large EKI waves when the applied static electric fields became relatively strong. The EKI waves were found to propagate both upstream and downstream in a random fashion as the strength of the applied static field becomes more significant, which results in more turbulent and chaotic fluid mixing in the Y-shaped microchannel.

A systematic study was also conducted to assess the effectiveness of manipulation EKI waves and resultant fluid mixing in the Y-shaped microchannel by adding alternative perturbations to the applied static electric fields. While the previous study of Shin et al. (2005) revealed that adding alternative perturbation to the applied static electric field can either enhance or suppress fluid mixing of three fluid streams in a cross-shaped microchannel, depending on the frequency of the alternative perturbation, the measurement results of the present study revealed that the fluid mixing of the two fluid streams in the Y-shaped microchannel can always be enhanced by adding the alternative perturbation. The fluid mixing process was found to be most enhanced when the frequency of the alternative perturbation is close to the natural shedding frequency of the convective EKI waves. Fluid mixing efficiency was found to increase almost linearly with the amplitude of the alternative perturbation when the perturbation amplitude is relatively small. The mixing efficiency was found to increase much more rapidly as the perturbation amplitude becomes relatively large.

Acknowledgments

The work described in the present study is the revision and extension of the paper presented at the “7th forum on the Transport Phenomena in Mixing” with the ASME Paper# FEDSM2007-37524. The support of National Science Foundation CAREER program to Hui Hu under award number of CTS-0545918 is gratefully acknowledged.

References

- [1] Nguyen, N.T. and Wu, Z., Micromixers – a review, *Journal of Micromechanics and Microengineering*. Vol.15, (2005), pp. r1-r16.
- [2] Mao, H., Yang, T. and Cremer, P. S. A microfluidic device with a linear temperature gradient for parallel and combinatorial measurements, *J. Am. Chem. Soc.* Vol. 124, (2002), pp.4432–4435.
- [3] Deshmukh, A. A., Liepmann, D. and Pisano, A. P., Characterization of a micro-mixing, pumping, and valving system, *Proc. Transducers'01, 11th Int. Conf. on Solid-State Sensors and Actuators* (Munich, Germany), (2001), pp.779–782.
- [4] Glasgow, I. and Aubry, N. Enhancement of microfluidic mixing using time pulsing. *Lab on a Chip*, Vol. 3, (2003), pp.114–20.
- [5] El Moctar, A. O., Aubry, N. and Batton, J., Electro-hydrodynamic micro-fluidic mixer, *Lab on a Chip*, Vol.3, (2003), pp.273–280
- [6] Deval, J., Tabeling, P. and Ho, C. M., A dielectrophoretic chaotic mixer, *Proc. MEMS'02, 15th IEEE Int. Workshop Micro Electromechanical System* (Las Vegas, Nevada), (2000), pp 36–39.
- [7] Bau, H. H., Zhong, J. and Yi, M., A minute magneto hydrodynamic (MHD), mixer *Sensors Actuators B*, Vol.79, (2001), pp.207–15.
- [8] Liu, R. H., Yang, J., Pindera, M., Z., Athavale M., and Grodzinski, P., Bubble-induced acoustic micromixing, *Lab on a Chip* Vol. 2, (2002), pp.151–157.
- [9] Chen, C. H. and Santiago, J. G., Electrokinetic flowinstability in high concentration gradient microflows”, *Proc.2002 Int. Mech. Eng. Cong. and Exp.* (New Orleans LA) vol. 1, (2002), paper no 33563.
- [10] Chen, C. H., Lin, H., Lele, S.K. and Santiago, J.G., Convective and absolute electrokinetic instability with conductivity gradients, *J. Fluid Mech.* Vol.524, (2005),

- pp.263-303.
- [11] Hoberg, J. F., and Melcher, J. R., Internal electrohydrodynamic instability and mixing of fluids with orthogonal field and conductivity gradients”, *J. Fluid. Mech.* Vol 73, (1976), pp.333-351.
 - [12] Baygents, J. C. and Baldessari, F. , Electrohydrodynamic instability in a thin fluid layer with an electrical conductivity gradient. *Phys. Fluids*, Vol.10, (1998), pp.301–311.
 - [13] Oddy, M. H., Santiago, J. G. and Mikkelsen, J. C., Electrokinetic instability micromixing”, *Anal. Chem.*, Vol 73, (2001), pp.5822-5832.
 - [14] Posner, J. D., and Santiago, J. D., Convective instability of electrokinetic flows in a cross-shaped microchannel, *J. Fluid Mech.*, Vol. 555, (2006), pp.1-42.
 - [15] Shin, S.M., Kang I.S. and Cho, Y.K., Mixing enhancement by using electrokinetic instability under time-periodic electric field, *J. Micromech. Microeng.* Vol 15, (2005), pp.445-462.
 - [16] Xia, Y., and Whitesides, G. M, Soft Lithography, *Angew. Chem. Int. Ed.*, vol. 37, (1998), pp.550-575.
 - [17] Schrum, K. F., Lancaster, J. M., Johnston, S. E. and Gilman, S. D., Monitoring electroosmotic flow by periodic photobleaching of a dilute, neutral fluorophore. *Analyt. Chem.* 72, (2000), pp.4317–4321.
 - [18] Inoue, S. and Spring, K., *Video Microscopy: The Fundamentals* . Plenum (1997).
 - [19] Hu, H., Saga, T., Kobayashi T. and Taniguchi, N., Analysis of a Turbulent Jet Mixing Flow by Using a PIV-PLIF Combined System, *Journal of Visualization*, Vol.7, No.1. (2004)., pp33-42.
 - [20] Johnson T. J., Ross D., and Locascio, L. E., Rapid microfluidic mixing, *Anal. Chem.* Vol. 74, No. 45 (2002), pp.45-51.
 - [21] Bryden, M. D. and Brenner, E., “Effect of laminar chaos on reaction and dispersion in eccentric annular flow”, *J. Fluid Mech.* Vol 325, (1996), pp.219–237.
 - [22] Lee S M, Im D J and Kang I S, “Circulating flows inside a drop under time-periodic nonuniform electric fields”, *Phys. Fluids*. Vol 12, 2000, pp1899.